INVESTIGATION OF NEUTRON SOURCE EFFECTS IN SUB-CRITICAL MEDIA AND APPLICATION TO A MODEL OF THE MUSE-4 EXPERIMENTS

P. Seltborg[1], R. Jacqmin
CEA/Cadarache - DER/SPRC/LEPh – Bat. 230
13 108 Saint-Paul-Lez-Durance, France
per@neutron.kth.se, Robert.Jacqmin@cea.fr

Keywords: MUSE-4, Neutron Source, Spallation, MCNP, MCNPX

ABSTRACT

Monte Carlo simulations have been performed to investigate the neutron source effects in a sub-critical media successively coupled to a *(d,d)*-source, a *(d,t)*-source and a spallation source. The investigations have focused on the neutron energy spectra in the fuel and on the source relative efficiency j^*. The calculations have been performed for three sub-critical configurations, representative of the coming MUSE-4 experiments.

The Monte Carlo codes MCNP and MCNPX have been used to compute j^*. j^* has been found to be low for the *(d,d)*-source (~1.35 compared to 1.0 for an average fission neutron), while considerably higher for the *(d,t)*-source (~2.15) and the spallation source (~2.35). The high value of j^* for the spallation source has been shown to be due to the fraction of high-energy neutrons (17 % of total source with $E_n > 20$ MeV) born from spallation, which contribute for 50 % to the total number of fission neutrons produced in the core. The variations of j^* with neutron importance have also been studied for some spherical configurations with a *(d,d)*- and a *(d,t)*-source. For the class of variations considered here, j^* was found to remain constant or increase only slightly in the interval $0.70 < k_{eff} < 0.996$.

1 INTRODUCTION

Accelerator Driven Systems (ADS) (Salvatores, 1999) are being investigated as a possible means for reducing the long-term radiotoxicity in the spent fuel from the nuclear industry. In principle, the sub-criticality of ADS allows for dedicated cores with a much higher concentration of minor actinides than what is acceptable in critical reactors. Those dedicated cores could achieve high transmutation rates. Research done on ADS indicates that a waste reduction factor of 50 to 100 is theoretically possible (Delpech et al, 1999).

---

[1] Permanent affiliation:
Department of Nuclear and Reactor Physics
Royal Institute of Technology
100 44 Stockholm, Sweden

The basic idea of ADS is to supply a sub-critical reactor core with neutrons generated by an intense external neutron source, usually from spallation reactions in a heavy metal target. This idea is being investigated in the MASURCA experimental facility at CEA Cadarache in the framework of the MUSE experiments (MUltiplication avec Source Externe). Different configurations and several different sub-critical levels are being studied (Salvatores, 1996; Soule, 1997; Lebrat, 1999).

The planned MUSE-4 experiments will not use a spallation source. Instead, a high-intensity pulsed neutron generator GENEPI, constructed by CNRS/ISN/Grenoble, will be used to accelerate a 250 keV deuteron beam towards either a deuterium target *(d,d)* or a tritium target *(d,t)* to produce well-characterized neutron sources *via* fusion reactions. *(d,d)*-reactions produce neutrons with energies between 2 and 3 MeV, while the *(d,t)*-reactions produce neutrons between 13 and 15 MeV.

The objective of the present study is to investigate neutron source effects in a MUSE-4-type sub-critical core coupled to a well-known *(d,d)*- or *(d,t)*-source, and to compare the results with those that would be obtained for a hypothetic spallation source coupled to the same core.

This investigation relies entirely on numerical simulations performed with the MCNP (Briesmeister, 2000) and MCNPX (Waters, 1999) Monte Carlo software packages. The two codes are essentially equivalent for neutron transport below 20 MeV. MCNP is used to simulate the production of the *(d,d)*- and *(d,t)*-sources, as well as neutron transport below 20 MeV. MCNPX is used to simulate the production of spallation neutrons and particle transport at all energies.

MCNP and MCNPX Monte Carlo models were set up in which a *(d,d)*-source, a *(d,t)*-source and a spallation source were successively coupled to three sub-critical configurations (Sc1, Sc2 and Sc3) representative of the upcoming MUSE-4 experiments.

A description of the MUSE-4 model, the calculation codes and the neutron sources used in this study is given in Section 2. In Section 3, the computed neutron energy spectra in the fuel are compared for the three different sources. In Section 4, we describe investigations of the neutron source efficiency j^*. The specific procedure used for calculating j^* with MCNP and MCNPX is described. The differences in the computed values of j^* are analysed, as well as the variations of j^* with neutron importance and reactivity.

2 DESCRIPTION OF THE MUSE-4 MODEL, CALCULATION TOOLS AND NEUTRON SOURCES USED IN THIS STUDY

2.1 The Muse-4 Model

Three homogeneous sub-critical configurations have been studied (Sc1, Sc2 and Sc3 with k_{eff} = 0.99, 0.97 and 0.95 respectively) representing three configurations planned in the MUSE-4 experiments. The geometry of the Sc2 model is shown in Fig. 1 below. The material compositions of the different regions are listed in Appendix A. The axial (z

direction) dimension of the fuel is 60.96 cm, except in a 21.2 cm wide channel above and below the lead buffer and the accelerator tube (in the y direction), where it was extended by 10.16 cm. The Na/SS reflector (Region 2) ends at z = ±61.76 cm. There is also a 10.16 thick axial shield (Region 3) above and below the Na/SS reflector. The overall dimensions of the whole model, including the reflector and the shields, are 159∗169.6∗143.84 cm.

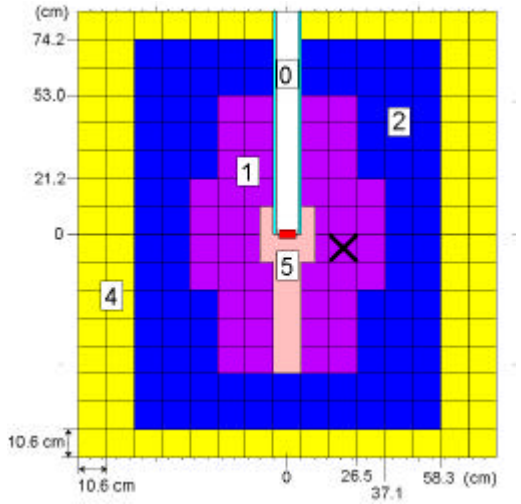

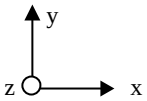

Region 0: Accelerator Tube
Region 1: Fuel
Region 2: Na/SS Reflector
Region 3: Axial Shield
Region 4: Radial Shield
Region 5: Lead Buffer

Fig. 1 *x-y Cross-sectional View of the MUSE-4 Sc2 Sub-Critical Configuration (k-eff = 0.97). The cross shows the position where the neutron spectra have been calculated, see Section 3.*

To obtain the two other sub-critical levels, Sc1 and Sc3, fuel cells were added or removed at the core periphery.

2.2 Description of the Calculation Codes

Calculations have been performed with MCNP-4C for models of the three MUSE-4 sub-critical configurations with the *(d,d)*- and *(d,t)*-sources. MCNPX was used to simulate the system with the spallation source. All simulations relied on the same evaluated nuclear data library, namely ENDF/B-VI.4.

MCNPX is the extended version of MCNP where the major capabilities of LAHET (Prael and Lichtenstein, 1989) and MCNP-4B (Briesmeister, 1997) have been merged together. In MCNP, particle transport relies entirely on nuclear data contained in externally supplied cross section tables (E_n < 20 MeV), which are derived from evaluated nuclear data files. In LAHET, on the other hand, particle transport is accomplished by using various theoretical physics models embedded in the code, covering the energy range up to several GeV. In MCNPX, the table-based data are used whenever they exist, as such data are known to yield the best results. When they do not exist, the code built-in physics models are used.

Several physics models are available for high-energy transport in MCNPX. In the first stage, in which the incident particles interact with the individual nucleons via particle-particle cross sections, the Intranuclear Cascade (INC) and Multistage Pre-

equilibrium (Prael, 1998) Models are used. The INC model used in this study is the Bertini package (Bertini, 1963). In the second stage the nucleus undergoes either evaporation (emitting neutrons and light ions) or fission, while in the final stage the excited nucleus decays by gamma emission, with energies described by a decay library (PHTLIB).

2.3 Description of the Sources

Three different neutron sources have been considered in this study: a *(d,d)*-, a *(d,t)*- and a spallation source. It should be noted that *(α,n)*- or spontaneous fission sources in the fuel have not been considered here.

2.3.1 The Fusion Sources used in MUSE-4

Two different fusion sources can be produced by the GENEPI neutron generator. 250 keV-deuterons are accelerated through the accelerator tube towards either a deuterium or a tritium target. The neutrons are emitted (the fusion reactions themselves are not simulated) from a point at the centre of the core (Fig. 2A). The energy of the emitted neutrons in the laboratory system (derived from basic kinematics) ranges from 2 to 3 MeV for the *(d,d)*-neutrons and from about 13 to 15 MeV for the *(d,t)*-neutrons, with a maximum emission probability density peaked in the forward direction. The source neutron energy spectrum and angular distribution used in this study are listed in Appendix B.

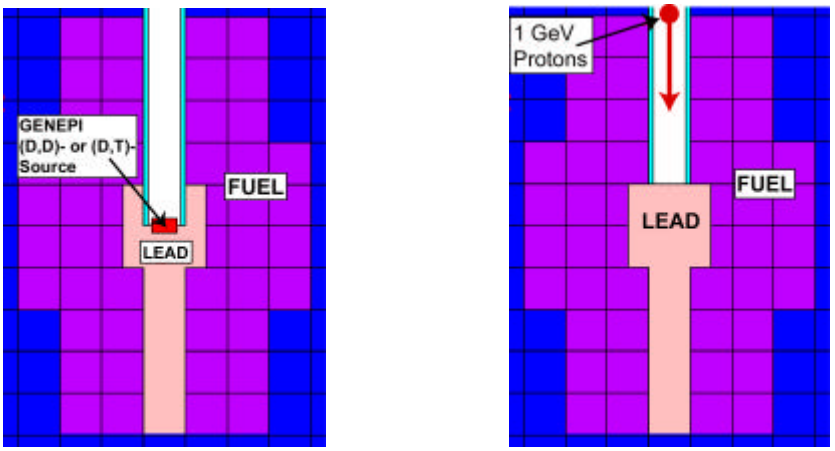

Fig. 2 *A) (d,d)- or (d,t)-Source Emitted from the GENEPI Neutron Generator at the Centre of the Core. B) 1 GeV Protons Accelerated Towards the Lead Buffer Creating Neutrons via Spallation Interactions. The generated neutrons are "frozen" and emitted as fixed source neutrons in a separate simulation.*

2.3.2 The Spallation Source

For the purpose of producing the spallation source for the numerical simulations, the lead buffer/target in the model was extended by one extra subassembly towards the proton beam, replacing part of the accelerator tube (Fig. 2B). This was done in order to

maximize neutron production near the centre of the core (the same position where the *(d,d)*- and the *(d,t)*-source neutrons are emitted).

The simulations with the spallation source were divided into two steps. A first simulation with the 1000 MeV proton beam (the protons were uniformly distributed across the beam of diameter 4 cm) impinging on the lead target, was performed with MCNPX. The properties, in terms of angular, energy and spatial distribution, of the primary neutrons born from the spallation interactions were recorded. In the second step, these primary neutrons were supplied to the MCNPX code as fixed source neutrons for separate simulations.

The spatial range of the primary neutrons was found to be rather limited, most neutrons being emitted within a 3 to 4 cm radius around the *z*-axis and within the first 30 cm axially, i.e., in the direction of the proton beam. The energy distribution of the neutrons produced from the 1000 MeV protons, integrated over all angles, is shown in Fig. 3 (neutrons created from secondary protons will have a slightly softer spectrum). We note that 17.3 % of the neutrons have energies higher than 20 MeV and 3.6 % of them higher than 150 MeV, and that these are mainly emitted in the forward direction of the incident proton beam. The effect of this high-energy fraction of neutrons on j^* will be discussed in Section 4.5.

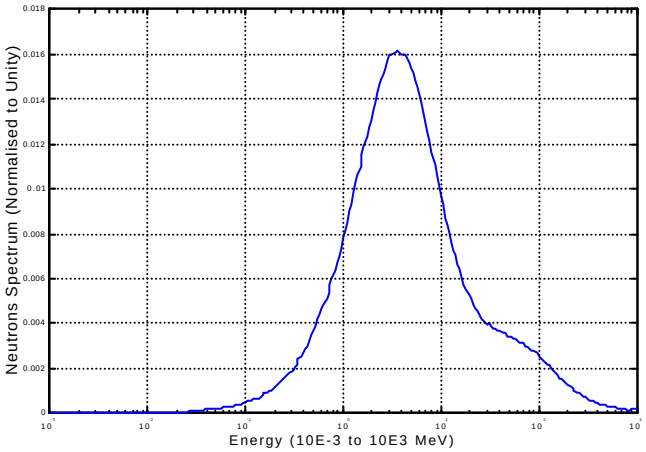

Fig. 3 *Spectrum of Primary Neutrons (Integrated over all Angles) born from 1000 MeV Protons Impinging on a very thin Target of Lead (Single Reaction).*

3 NEUTRON SPECTRA IN THE MUSE-4 CORE

The Sc3 sub-critical configuration of the MUSE-4 model with k_{eff} = 0.95 was simulated. The neutron energy spectra resulting from the three different sources were calculated in the subassembly centred at 21.2 cm from the centre of the core, indicated with a cross in Fig. 1. The neutron spectra of the other sub-critical states (Sc1 and Sc2) are not shown here, since they are very similar to the spectra of Sc3.

It is seen in Fig. 4 that the three spectra at this position are very similar to each other and that they are largely dominated by the fission multiplication in the fuel. The

two dips in the neutron fluxes caused by the resonances in sodium (~ 3 keV) and oxygen (~ 0.4 MeV) can be seen. The fraction of neutrons still having their initial (source) energy is very small (but should not automatically be disregarded) – about 0.2 % of the *(d,t)*-neutrons are still in the 14 MeV peak and 0.1 % of the spallation neutrons have energies above 20 MeV. Hence, we conclude that, for the purpose of computing neutron spectrum weighted quantities, the presence of the external sources can be considered "forgotten" beyond a few centimetres into the fuel.

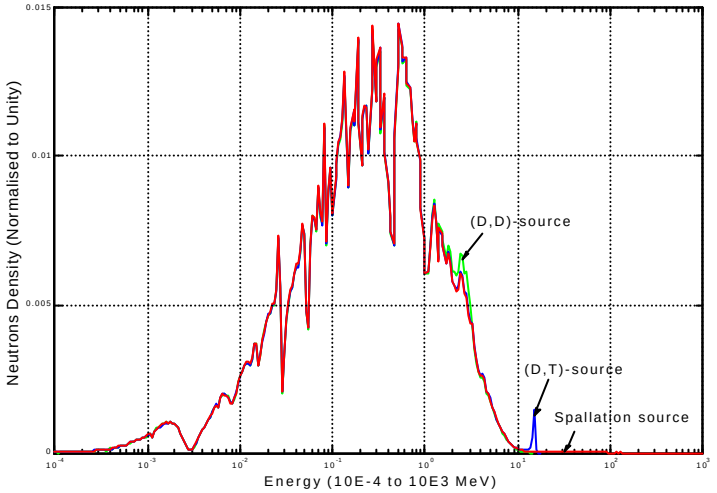

Fig. 4 *MUSE-4 Neutron Energy Spectra in the Subassembly Centred at x=21.2 cm, y=-5.3 cm, Resulting from the three Different External Sources.*

4 SOURCE EFFICIENCY

The relative efficiency (j^*) of the source neutrons was determined for the three different sources and for the three different sub-critical configurations of the MUSE-4 model.

4.1 Definition of j^*

The neutron flux distribution in a sub-critical core is the solution of the inhomogeneous balance equation:

$$\mathbf{A} f_s = \mathbf{F} f_s + S \qquad (1)$$

where $\mathbf{F}$ is the fission production operator, $\mathbf{A}$ is the net neutron loss operator and S is the external source. The quantity j^*, which represents the relative efficiency of external source neutrons, is defined as the ratio of the average importance of the external source neutrons to the average importance of the fission neutrons (Salvatores, 1999), i.e.:

$$j^* = \frac{\dfrac{< f_0^*, S >}{< S >}}{\dfrac{< f_0^*, \mathbf{F} f_s >}{< \mathbf{F} f_s >}} \qquad (2)$$

where $\boldsymbol{f}_0^*$ = The adjoint flux (the everywhere positive solution of $\boldsymbol{A}^* \boldsymbol{f}_0^* = \frac{1}{k_{eff}} \boldsymbol{F}^* \boldsymbol{f}_0^*$) which provides a measure of neutron importance.

$\langle \boldsymbol{F} \boldsymbol{f}_s \rangle$ = Total production of neutrons by fission.

$\langle S \rangle$ = Total production of neutrons by the external source.

In the above formula, the brackets imply integration over space, angle and energy.

As some of the integrals in Eq. (2) cannot be directly calculated with MCNP and MCNPX, another procedure was sought to compute $\boldsymbol{j}^*$. By using the balance equation (Eq. 1), the properties of the adjoint flux $\boldsymbol{f}_0^*$, the $\boldsymbol{A}$, $\boldsymbol{F}$ operators and their adjoints $\boldsymbol{A}^*$, $\boldsymbol{F}^*$, the source efficiency can be expressed equivalently as

$$j^* = \left(\frac{1}{k_{eff}} - 1 \right) \cdot \frac{\langle \boldsymbol{F} f_s \rangle}{\langle S \rangle} \qquad (3)$$

Eq. (3) is a simple formula relating the total fission neutron production $\langle \boldsymbol{F} \boldsymbol{f}_s \rangle$ to the external source, $\boldsymbol{j}^*$ and reactivity ($1 - 1/ k_{eff}$). It shows that, for given values of k_{eff} and $\langle S \rangle$, the larger $\boldsymbol{j}^*$ the larger the fission power produced in the system.

The quantities in the right hand side of Eq. (3) are standard outputs from MCNP and MCNPX. For simplicity, the production terms will be labelled only F and S in the sequel.

4.2 Estimation of the Statistical Error in $\boldsymbol{j}^*$

To get an estimate of the statistical uncertainty in the source efficiency, assume that the errors of F and S are $\boldsymbol{D}F$ and $\boldsymbol{D}S$ and apply the formula for "propagation of error" (Eq. 4)

$$\Delta f(x_1, x_2, \ldots) = \sqrt{\left(\frac{\partial f}{\partial x_1} \Delta x_1 \right)^2 + \left(\frac{\partial f}{\partial x_2} \Delta x_2 \right)^2 + \ldots + r_{12} \cdot \frac{\partial f}{\partial x_1} \Delta x_1 \cdot \frac{\partial f}{\partial x_2} \Delta x_2 + \ldots} \qquad (4)$$

The correlation constant $\boldsymbol{r}$ could be either positive or negative – negative if k_{eff} and F are correlated and positive if they are anti-correlated. However, as a first approximation, $\boldsymbol{r}$ may be assumed to be zero. With the derivatives $\frac{\partial \boldsymbol{j}^*}{\partial k_{eff}}$, $\frac{\partial j^*}{\partial F}$ and $\frac{\partial j^*}{\partial S}$ inserted in Eq. (4) an expression for the relative error in $\boldsymbol{j}^*$ can be obtained:

$$\left(\frac{\Delta j^*}{j^*} \right)^2 \approx \left(\frac{1}{1 - k_{eff}} \cdot \frac{\Delta k_{eff}}{k_{eff}} \right)^2 + \left(\frac{\Delta F}{F} \right)^2 + \left(\frac{\Delta S}{S} \right)^2 \qquad (5)$$

Eq. 5 will be used in the subsequent sections to estimate the statistical uncertainty in $\boldsymbol{j}^*$.

4.3 Calculations of j^* for the MUSE-4 Model

The multiplication factor k_{eff} and the total number of neutrons produced by fission (F) were calculated for the three different sources and the three different sub-critical configurations. F was automatically normalised per source neutron, so S was always equal to 1. The source efficiency was calculated according to Eq. (3) and the corresponding statistical errors (±1 standard deviation) according to Eq. (5). All results including error estimations are listed in Table 1.

Table 1 *MCNP/MCNPX Results for the MUSE-4 Sc1, Sc2 and Sc3 Configurations.*

	Source	k_{eff}	F	j^*
Sc1	**(D,D)-Source**	0.99045 (± 8 pcm)	140.2 (± 1.6 %)	**1.35 (± 0.024)**
	(D,T)-Source		223.2 (± 1.7 %)	**2.15 (± 0.040)**
	Spallation Source	0.99040 (± 8 pcm)	248.6 (± 1.8 %)	**2.41 (± 0.047)**
Sc2	**(D,D)-Source**	0.97007 (± 14 pcm)	44.2 (± 0.9 %)	**1.36 (± 0.015)**
	(D,T)-Source		69.9 (± 1.0 %)	**2.16 (± 0.024)**
	Spallation Source	0.96992 (± 15 pcm)	76.6 (± 1.1 %)	**2.37 (± 0.028)**
Sc3	**(D,D)-Source**	0.94982 (± 14 pcm)	25.4 (± 0.6 %)	**1.34 (± 0.009)**
	(D,T)-Source		40.1 (± 0.5 %)	**2.12 (± 0.013)**
	Spallation Source	0.94993 (± 15 pcm)	44.2 (± 0.7 %)	**2.33 (± 0.018)**

The energy of the *(d,d)*-source neutrons (2-3 MeV, see Appendix B) is only slightly larger than the average energy of a neutron produced by fission. The j^* value for the *(d,d)*-source is therefore expected to be equal or slightly larger than 1, which is indeed the case.

In the case of the *(d,t)*-source, the reason for the higher values of j^* is the larger fission rate, part of which coming from fissions induced by the neutrons multiplied by *(n,2n)*-reactions in the lead buffer. It is seen in Table 1 that the number of fission neutrons per source neutron is large, approximately 58 % larger than for the *(d,d)*-source. It is also seen in Fig. 5 that the *(n,2n)*-cross section in lead has a threshold at about 7 MeV, which is the reason why this reaction is insensitive to the *(d,d)*-source neutrons. At 14 MeV the value of the lead *(n,2n)*-cross section is about 2 barns, which is comparable to the fission cross section in Pu-239 and in U-238.

Concerning the spallation source neutrons, the values of j^* obtained in the simulations are somewhat higher than for the *(d,t)*-source. This is due to the fraction of neutrons having a very high energy (see Section 2.3.2). Most of the neutrons from the spallation process are born with an energy lower than the *(n,2n)*-cross section threshold in lead, but the neutrons with very high energy contribute significantly to j^*, as will be shown in Section 4.5.

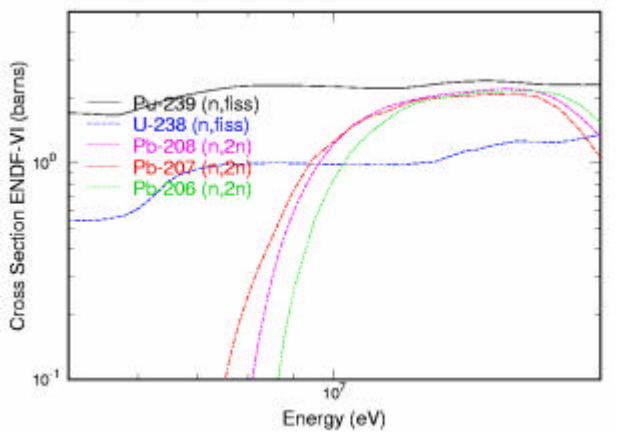

Fig. 5 *Neutron Microscopic Cross Sections for Pu-239 Fission, U-238 Fission and (n,2n)-Reactions in Pb-206, -207,-208. (ENDF/B-VI.4)*

It is also seen in Table 1 that, for all three sources, j^* remains approximately constant or increases slightly as k_{eff} increases. This trend will be further discussed in the following section.

4.4 Dependence of j^* on Neutron Importance and k_{eff}

The dependence of the source efficiency on neutron importance f_0^* was investigated for a wider range of sub-criticality (k_{eff} = 0.70 to 0.996), for a *(d,d)*- and a *(d,t)*-source, using a spherical model consisting of a buffer core (lead or U-238 with r =10 cm) and MUSE-4 type fuel. Only a limited class of importance variations was considered. The results are plotted in Fig. 6.

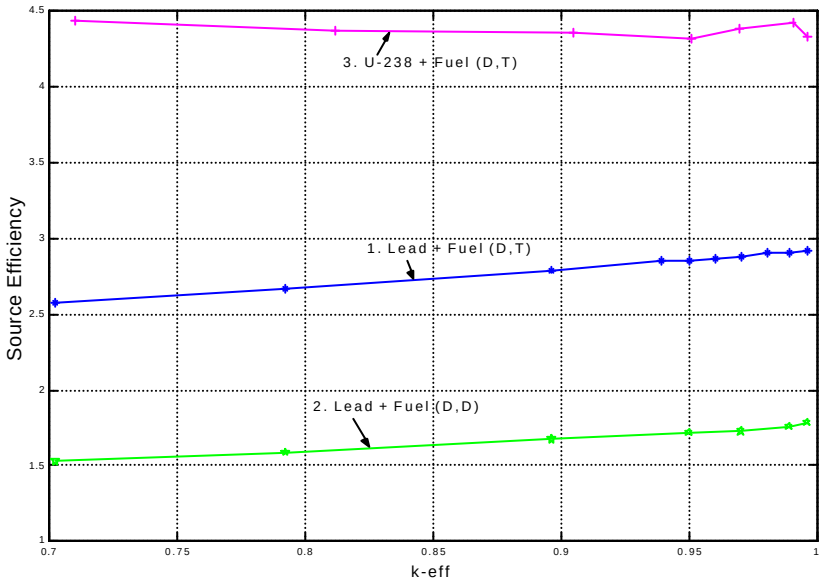

Fig. 6 *j^* versus k_{eff} for Spherical Configurations with a Buffer of Lead or U-238 (r=10 cm) and MUSE-4 type Fuel, Coupled to a (d,d)- and a (d,t)-Source. The neutron importance and k_{eff} were changed by varying the fuel radius from about 48 cm (k_{eff} » 0.70) to 68 cm (k_{eff} » 0.996).*

Instead of plotting the ratio j^* / ($1/k_{eff} - 1$) versus k_{eff} which would reflect the rapid increase of $< \Phi f_S > / < S >$ (and therefore of the fission power) as k_{eff} approaches unity, we focused instead on the behaviour of j^* versus k_{eff}. The neutron importance (and therefore k_{eff}) was varied by changing the outer radius of the fuel from approximately 48 to 68 cm. It is seen in Fig. 6 that j^* shows the same almost constant or slightly increasing trend in the interval k_{eff} = 0.95 to 0.99, for the spherical configurations with the lead buffer, as already observed for the MUSE-4 model.

The first case (Case 1) is a sphere consisting of a lead core surrounded by fuel with approximately the same material composition as listed in Table 3. j^* increases slightly but constantly in the interval k_{eff} = 0.70 to 0.996. The importance of the *(n,2n)*-effect is also demonstrated by replacing the *(d,t)*-source by a *(d,d)*-source (Case 2), which results in significantly lower values of j^*. The curve shows the same increasing trend as for the *(d,t)*-source.

In Case 3, when the lead buffer at the centre of the sphere is replaced by U-238, a large increase in j^* occurs at all sub-criticality levels because of U-238 fissions. The same increasing trend as with the lead buffer is not observed here as j^* remains nearly constant.

The statistical errors of the j^* values are rather small in the range $0.70 \leq k_{eff} \leq 0.99$ – less than 1 % (±1 standard deviation), while around 2.5 % for the very last point (k_{eff} = 0.996). In the absolute vicinity of criticality ($k_{eff} \geq 0.996$) the computation time for calculating j^* grows too large to obtain reliable results.

We conclude that the variations of j^* with neutron importance are rather small in the investigated range $0.70 \leq k_{eff} \leq 0.996$.

4.5 Decomposition of the Spallation Source

Most reactor code simulations only take into account neutrons with energies lower than 20 MeV. However, a significant fraction of the neutrons produced by spallation have energies higher than 20 MeV (see Fig. 3). The contribution of those high-energy neutrons to the source efficiency needs to be investigated. For this, the spallation source was artificially split into two "low-energy" bins (S_1 from 0 to 5 MeV and S_2 from 5 to 20 MeV) and two "high-energy" bins (S_3 from 20 to 150 MeV and S_4 from 150 to 1000 MeV). The study was performed for the third sub-critical level Sc3 (k_{eff} = 0.95) of the MUSE-4 model.

In order to derive a formula for the low- and high-energy contributions to the source efficiency, we start from Eq. (3), applied to each source bin

$$j_i^* = \left(\frac{1}{k_{eff}} - 1 \right) \cdot \frac{< \Phi f_i >}{< S_i >} \qquad (6)$$

where f_i = Flux resulting from each source bin ($S_1 \rightarrow f_1$, $S_2 \rightarrow f_2$ etc.).

Since $< \nu f_T >= \sum_{i=1}^{4} < \nu f_i >$, the following relationship for the decomposition of ν^* is readily obtained

$$\nu_T^* = \sum_{i=1}^{4} \nu_i^* \cdot \frac{< S_i >}{< S_T >} \qquad (7)$$

where ν_T^* = Efficiency of the total source.
ν_i^* = Efficiency of each source bin alone.

The ν_i^* results obtained from the Monte Carlo simulations are listed in Table 2. As expected, for the first low-energy bin, ν_i^* is low (ν_1^*=1.25) and close to the value obtained for the *(d,d)*-source. For the second bin, it is found to be higher (ν_2^*=1.71) since many of the neutrons have energies above the lead *(n,2n)*-cross section threshold. For the two high-energy parts, ν_i^* is very high (ν_3^*=4.58 and ν_4^*=14.4), which is the consequence of fissions induced by neutrons born from *(n,xn)*-reactions and spallation interactions.

Table 2 *MCNPX Results for the Sc3 MUSE-4 Model (k_{eff} = 0.94993) Obtained from the Decomposition of the Spallation Source.*

Source Bin	Energy limits (MeV)	$\frac{< S_i >}{< S_T >}$ A	$\frac{< \nu f_i >}{< S_i >}$ B	ν_i^*	$\nu_i^* \cdot \frac{< S_i >}{< S_T >}$ C
S_1	0 - 5	0.559	23.7	1.25	0.699 (30 %)
S_2	5 - 20	0.268	32.5	1.71	0.458 (20 %)
S_3	20 - 150	0.137	86.9	4.58	0.627 (27 %)
S_4	150 - 1000	0.036	273.1	14.4	0.518 (23 %)
					Sum = 2.30
S_T D	0 - 1000	1.0	44.2	2.33	

The superscripts A, B, C and D in Table 2 stand for:

A: Fraction of the total number of source neutrons in each energy bin (compare Fig. 3).
B: Neutrons produced by fission in the core.
C: Contribution to total ν^* (Product of column 3 and 5).
D: Simulation with the total source, identical as for Sc3 in Table 1.

It is also seen in Table 2 that the two high-energy parts (17.3 % of the total number of source neutrons), contribute for about 50 % of the total ν^*, and the highest energy part alone (3.6 % of the total number of source neutrons) for more than 20 %. The sum of the contributions to ν^* from the four different parts in the rightmost column, according to Eq. (7), is 2.30, which is in good agreement with the value obtained from the simulation with the total source (ν_T^*=2.33). The statistical 1σ error estimates in the ν^* values are less than 1 %.

The rather high average number of fission neutrons produced per source neutron for the two high-energy bins (87 and 273 respectively) might seem surprising at first. The explanation for this is that most of the high-energy neutrons from the spallation source

have already been multiplied in the lead (via secondary spallation and *(n,xn)*-reactions) *before* they enter into the fuel. Each of them gives birth to a number of lower-energy neutrons, which then leak out of the lead and induce fission chain reactions in the fuel. Additional simulations in which the lead target alone was kept showed that only about 5 % of the neutrons leaking out of the lead have energies higher than 20 MeV and about 1 % of them higher than 150 MeV.

We conclude that, although neutron transport in the fuel is largely dominated by neutrons with low energy ($E_n < 20$ MeV) which can be well simulated with a number of classical calculation codes such as MCNP, the importance of the high-energy contribution to j^* indicates the need for further investigating the effects from high-energy spallation neutrons. This could be made easier by extending the capabilities of existing neutronics codes, in particular deterministic codes, for studying high-energy (20-150 MeV) neutron transport.

5 CONCLUSIONS

Numerical simulations have been performed with MCNP and MCNPX to investigate the neutronic properties of a sub-critical core representative of the up-coming MUSE-4 experiments, alternatively coupled with a *(d,d)*-source, a *(d,t)*-source and a spallation source. The source-plus-core systems have been studied in terms of neutronic spectra and efficiency (j^*) in three different sub-critical configurations (k_{eff} = 0.99, 0.97, 0.95).

The computed neutron spectra in all cases show that fission multiplication dominates at distances past a few centimetres into the fuel. This implies that, for the purpose of ADS core studies, the presence of the source may be ignored in the calculation of spectrum-weighted quantities, except possibly in the immediate vicinity of the external source.

The relative efficiency of the *(d,d)*-source is somewhat higher than 1 (~1.35). For the *(d,t)*-source, it is much larger, around 2.15. This significantly larger value is due to the *(n,2n)*-multiplication in lead (with an energy threshold at about 7 MeV) and the induced fissions. To analyse the high value of j^* obtained for the spallation source (~2.35), the source was artificially split into four different energy bins and the efficiency of each bin was determined. It was found that these two high-energy bins ($E_n > 20$ MeV) contribute for about 50 % to j^* and to the total number of fission neutrons produced in the core. This can be explained by the fact that primary neutrons born with high energy from spallation give birth to a large number of lower-energy neutrons, which in turn induce fissions. This rather high fraction indicates the need for extending reactor analysis code capabilities above 20 MeV for more detailed investigations of high-energy spallation neutron effects.

The variations of j^* with neutron importance (and reactivity) was also investigated for different spherical configurations. It was found that j^* remains approximately constant or increases slightly in the interval $0.70 < k_{eff} < 0.996$.

AKNOWLEDGEMENTS

This research work is supported and partly funded by SKB AB, Sweden, the Swedish Centre of Nuclear Technology, and the European Commission, DGRTD, under Contract # FIKW-CT-2000-00063.

REFERENCES

Bertini, H. W., 1969. Phys. Rev. 131, 1801.

Briesmeister, J.F. MCNP^{TM} – A General Monte Carlo N-Particle Transport Code – Version 4B. LANL/Los Alamos, LA-12625-M, March, 1997.

Briesmeister, J.F. MCNP^{TM} – A General Monte Carlo N-Particle Transport Code – Version 4C. LANL/Los Alamos, LA-13709-M, April 10, 2000.

Delpech, M. et al., 1999. The Am and Cm Transmutation – Physics and Feasability. Global'99.

Lebrat, J.F. et al., 1999. Experimental investigation of multiplying sub-critical media in presence of an external source operating in pulsed or continuous mode: The MUSE-3 experiment. ADTTA'99.

Prael R.E., Lichtenstein H. User Guide to LCS: The LAHET Code System. Los Alamos National Laboratory, LA-UR-89-3014, September 15, 1989.

Prael R.E., Bozoian M. Adaptation of the Multistage Pre-equilibrium Model for the Monte Carlo Method (I). Los Alamos National Laboratory Report LA-UR-88-3238, September 1998.

Salvatores, M., Martini, M., Slessarev, I. MUSE-1: A first experiment at MASURCA to validate the physics of sub-critical multiplying systems relevant to ADS. Kalmar, Sweden, June 3-7, 1996.

Salvatores, M., 1999. Accelerator Driven Systems (ADS), Physics Principles and Specificities. J. Phys. IV France 9, pp. 7-17 –7-33.

Soule, R., Salvatores, M., Jacqmin, R., 1997. Validation of neutronic methods applied to the analysis of fast sub-critical systems: The MUSE-2 experiments. Global'97, page 639.

Waters, L.S. MCNPX^{TM} User´s Manual – Version 2.1.5. Los Alamos National Laboratory, November 14, 1999.

APPENDIX A

Table 3 *Material Composition for the Different Homogeneous Regions of the MUSE-4 Model.*

	Atomic Density of Materials [10^{24} atoms/cm^3]					
Isotope	**Fuel**	**Na/SS Reflector**	**Axial Shield**	**Radial Shield**	**Lead Buffer**	**Accelerator Tube**
C	2.75e-05	1.90e-05	1.64e-05	1.47e-03	1.64e-05	9.32e-05
O-16	1.44e-02	-	-	-	-	-
Na-23	9.32e-03	4.66e-03	-	-	-	-
Al-27	-	-	-	-	-	1.46e-02
Si	1.00e-05	1.18e-03	1.54e-03	2.98e-05	2.98e-05	1.15e-04
Cr-52	1.62e-03	1.02e-02	1.30e-02	8.00e-04	7.58e-04	1.75e-03
Cr-53	1.84e-04	1.15e-03	1.47e-03	9.07e-05	8.59e-05	1.98e-04
Mn-55	1.24e-04	8.33e-04	1.07e-03	5.83e-04	3.61e-05	1.75e-04
Fe-54	4.16e-04	2.74e-03	3.50e-03	4.70e-03	1.97e-04	4.58e-04
Fe-56	6.47e-03	4.26e-02	5.45e-02	7.30e-02	3.06e-03	7.01e-03
Ni-58	6.49e-04	3.48e-03	4.42e-03	7.43e-04	2.64e-04	6.78e-04
Ni-60	2.50e-04	1.34e-03	-	2.86e-04	1.02e-04	2.61e-04
Pb-206	-	-	-	-	7.72e-03	4.09e-03
Pb-207	-	-	-	-	6.69e-03	3.54e-03
Pb-208	-	-	-	-	1.59e-02	8.40e-03
Bi-209	-	-	-	-	1.50e-06	-
U-235	1.75e-05	-	-	-	-	-
U-238	5.26e-03	-	-	-	-	-
Pu-239	1.52e-03	-	-	-	-	-
Pu-240	3.71e-04	-	-	-	-	-
Pu-241	2.84e-05	-	-	-	-	-
Pu-242	1.33e-05	-	-	-	-	-
Am-241	4.95e-05	-	-	-	-	-

APPENDIX B

Table 4 *Laboratory-system Angular and Energy Dependence (Derived from Basic Kinematics) of the (d,d)- and the (d,t)-Source Neutrons Emitted at the Centre of the Core, Resulting from the GENEPI 250 keV Deuterons Impinging on a Deuterium/Tritium Target.*

	(D,D)-reaction		(D,T)-reaction	
Angle	**Energy**	**Emission probability density**	**Energy**	**Emission probability density**
0	3.050	5.250%	15.12	4.924%
9	3.042	5.243%	15.10	4.922%
18	3.020	5.223%	15.07	4.916%
27	2.984	5.192%	15.00	4.906%
36	2.935	5.150%	14.92	4.893%
45	2.876	5.098%	14.82	4.876%
54	2.808	5.038%	14.70	4.856%
63	2.734	4.970%	14.57	4.834%
72	2.656	4.899%	14.43	4.811%
81	2.576	4.825%	14.28	4.786%
90	2.496	4.750%	14.13	4.760%
99	2.419	4.676%	13.98	4.735%
108	2.346	4.605%	13.83	4.711%
117	2.279	4.538%	13.70	4.688%
126	2.219	4.478%	13.58	4.667%
135	2.167	4.425%	13.47	4.648%
144	2.123	4.380%	13.37	4.632%
153	2.089	4.344%	13.30	4.619%
162	2.064	4.318%	13.25	4.610%
171	2.049	4.302%	13.21	4.604%
180	2.044	4.297%	13.20	4.602%